Orthopaedic Surgery

CLINICAL ARTICLE OPEN ACCESS

Biomechanical Effects of Zero-P Height on Anterior Cervical Discectomy and Fusion: A Finite Element Study

Cheng-yi Huang[1] | Jun-bo He[1] | Xing-Jin Wang[1] | Ting-kui Wu[1] | Bei-yu Wang[1] | Jin Xu[2] | Hao Liu[1]

[1]Department of Orthopedics, Orthopedic Research Institute, West China Hospital, Sichuan University, Chengdu, China | [2]Department of Pain Treatment, Tianjin Hospital, Tianjin, China

Correspondence: Jin Xu (doctorjinjin@163.com) | Hao Liu (liuhaohxyy@163.com)

Received: 9 September 2024 | **Revised:** 4 January 2025 | **Accepted:** 13 January 2025

Funding: This work was supported by research grants from the Cadre Health Research Project of Sichuan Province (Grant no ZH2023-105 to Hao Liu); the National Natural Science Foundation of China (Grant no 82302785 to Ting-kui Wu); the 1.3.5 project for Postdoctoral Foundation of West China Hospital of Sichuan University (Grant no 2023HXBH080 to Ting-kui Wu).

Keywords: anterior cervical discectomy and fusion | biomechanics | finite element analysis | zero-P

ABSTRACT

Objective: The principle of selecting a Zero-P implant of an appropriate height remains a topic of debate, particularly when similarly sized implants seem to appropriately fit the intervertebral space. Thus, this study compared the biomechanical performance of smaller and larger Zero-P implants within an appropriate height range with that of oversized Zero-P implants for anterior cervical discectomy and fusion (ACDF).

Methods: A three-dimensional finite element (FE) model of the C2–C7 cervical spine was constructed and validated. The implants were categorized as smaller (6 mm), larger (7 mm), and oversized (8 mm) according to the average intervertebral height and implant specifications. Thus, the following four FE models were constructed: the intact cervical spine model (M1), the 6 mm model (M2), the 7 mm model (M3), and the 8 mm (M4) Zero-P implant C5/6 segment ACDF surgical model. Then, a pure moment of 1.0 N·m combined with a follower load of 75 N was applied at C2 to simulate flexion, extension, lateral bending, and axial rotation.

Results: The results indicated that the maximum stress on the vertebral body, intervertebral disc, and facet joints under self-weight increased with increasing Zero-P height. Under six different loading conditions, the maximum stress on the vertebral body in the surgical segment of the M4 model was generally greater than that in the M2 and M3 models. Following an increase in the height of the implant from 6 mm to 8 mm, the maximum stress increased, and the intervertebral disc stress of both segments reached its peak in the M4 model. In the M4 model, the implant experienced the highest stress, whereas the M2 model exhibited the lowest stress on the implant under both self-weight and loading conditions. Furthermore, the stress on the posterior facet joints of the surgical segment increased with increasing Zero-P height. The range of maximum stress on the posterior facet joints for the M3 model was situated between that of the M2 and M4 models.

Conclusion: In summary, after determining the appropriate height range for the implant in accordance with the mean height of the intervertebral space, opting for a larger size appears to be more advantageous. This approach helps maintain the height of the

Abbreviations: ACDF, anterior cervical discectomy and fusion; ALL, anterior longitudinal ligament; CL, capsular ligament; CT, computed tomography; DICOM, Digital Imaging and Communications in Medicine; FE, finite element; FSU, functional spinal unit; IL, interspinous ligament; LF, ligamentum flavum; PLL, posterior longitudinal ligament; ROM, range of motion; SL, supraspinous ligament.

Cheng-yi Huang and Jun-bo He contributed equally to this work and should be considered co-first authors.

We declare that all authors listed meet the authorship criteria according to the latest guidelines of the International Committee of Medical Journal Editors. All authors agree to the final submitted manuscript.

intervertebral space and provides greater stress, promoting a tighter fit between the upper and lower endplates and the Zero-P. This tighter fit is crucial for maintaining spinal stability, enhancing the early bony fusion rate, and potentially leading to better postoperative outcomes.

1 | Introduction

Anterior cervical discectomy and fusion (ACDF) is widely performed for the treatment of cervical degenerative disc disease [1–3]. The intervertebral cage, which is used to maintain intervertebral space height and promote postoperative bony fusion, has remained a topic of research aimed at enhancing the efficacy of ACDF [4, 5]. Furthermore, the utilization of the anterior cervical plate improves stability immediately after surgery, promotes bone fusion, and significantly reduces the risk of cage subsidence [6, 7]. Consequently, the combined use of a plate and a cage is now regarded as the standard approach in ACDF procedures [1, 7].

Nonetheless, numerous complications can arise from the use of the anterior cervical plate, primarily due to excessive contact with the prevertebral soft tissue and increased stress on adjacent segments [8–10]. Hence, zero-profile devices, such as the Zero-P system (Synthes, Oberdorf, Switzerland), which has the functionality of both an anterior cervical plate and a cage, were developed [11, 12]. Although the Zero-P device and a traditional plate can achieve similar clinical outcomes, the incidence of complications is lower with the Zero-P device than with a traditional plate [13, 14]. The optimal height of the cage used for ACDF remains a topic of discussion considering that implants with different heights can be implanted in the same intervertebral space [15, 16]. The selection of an implant with an appropriate height plays an important role in clinical and radiological outcomes considering that a fusion cage that is either too tall or too short can alter the height of both the intervertebral space and the intervertebral foramen [15–17]. This can adversely affect the biomechanics of stress distribution of the surgical segment and the adjacent segments, potentially increasing the incidence of complications such as adjacent segment degeneration or subsidence [15, 16]. Given the widespread use of Zero-P devices, it is imperative to explore the biomechanical impact of the height of Zero-P implants on ACDF.

To our knowledge, there are no reports regarding this topic. Therefore, we explored the biomechanical effects of the Zero-P implant height on ACDF through finite element analysis. By conducting this study, we aimed to establish a theoretical foundation for selecting the optimal Zero-P implant. This will assist surgeons in selecting the optimal Zero-P implant model for ACDF.

2 | Methods

2.1 | Construction of the Cervical Spine Model and Instruments

A nonlinear three-dimensional finite element (FE) model of cervical spine segments (C2–C7) was developed and validated in our previous study [18]. The computed tomography (CT) images were obtained from a healthy 23-year-old female volunteer (161 cm, 53 kg). The slice thickness was 0.75 mm, and the interval was 0.69 mm. A SOMATOM Definition AS+ scanner (Siemens, Germany) was used for image acquisition. A total of 393 axial CT images were exported in Digital Imaging and Communications in Medicine (DICOM) format. The C2–C7 spine FE models were constructed using Mimics 17.0 software (Materialize Corporation, Belgium). Afterward, the models were refined through denoising, surfacing, and smoothing by Geomagic Studio 2015 (Raindrop Geomagic Inc., USA). The models (Figure 1) were subsequently loaded into Hypermesh 14.0 (Altair Corporation, USA) to prepare the mesh structures. ABAQUS 6.9.1 (Dassault Systèmes Corporation) was used to define the boundary conditions and carry out the analysis.

According to previous studies [19–21], the cortical bone and bony endplates were constructed such that the shell covering the cancellous bone was 0.4 mm thick. The intervertebral disc was divided into the annulus fibrosus and nucleus at a volume ratio of 6:4. Annulus fibers, which make up approximately 19% of the annulus fibrosus volume, encircle the ground material at an angle between 15° and 30° with respect to the transverse plane. The endplates and intervertebral disc were designated as tie connections. The cartilage layer covering the 0.5 mm facet joint space had nonlinear surface-to-surface contact. Frictionless contact was established between the facet joints' articular surfaces. In addition, the ligaments, such as the anterior longitudinal ligament (ALL), posterior longitudinal ligament (PLL), ligamentum flavum (LF), interspinous ligament (IL), supraspinous ligament (SL), and capsular ligament (CL), were set as tension-only truss elements and attached to the corresponding vertebrae. The material properties are shown in Table 1. The numbers of nodes and elements of the cervical spine model are summarized in the Supporting Information—Table S1.

A Zero-P system, 15 mm wide and 16 mm long, was used for ACDF. The C5/6 level was selected for Zero-P implantation according to previous studies and clinical data [19, 20, 22]. On the basis of the intact cervical spine model (M1), the anterior height of the C5/6 intervertebral space was 7.2 mm, the middle height was 6.4 mm, the posterior height was 6.3 mm, and the initial height of the Zero-P implant was 6 mm. Furthermore, according to the average intervertebral height and Zero-P implant specifications, the implant measuring 6 mm in height was considered the smaller implant and the implant measuring 7 mm in height was considered the larger implant. The implant measuring 8 mm in height was considered the oversized implant. Three surgical models were subsequently constructed: the 6 mm Zero-P implant C5/6 segment ACDF surgical model (M2), the 7 mm Zero-P implant C5/6 segment ACDF surgical model (M3), and the 8 mm Zero-P implant C5/6 segment ACDF surgical model (M4). The self-tapping screws were 16 mm in length. The cage was filled with frictionless cancellous bone.

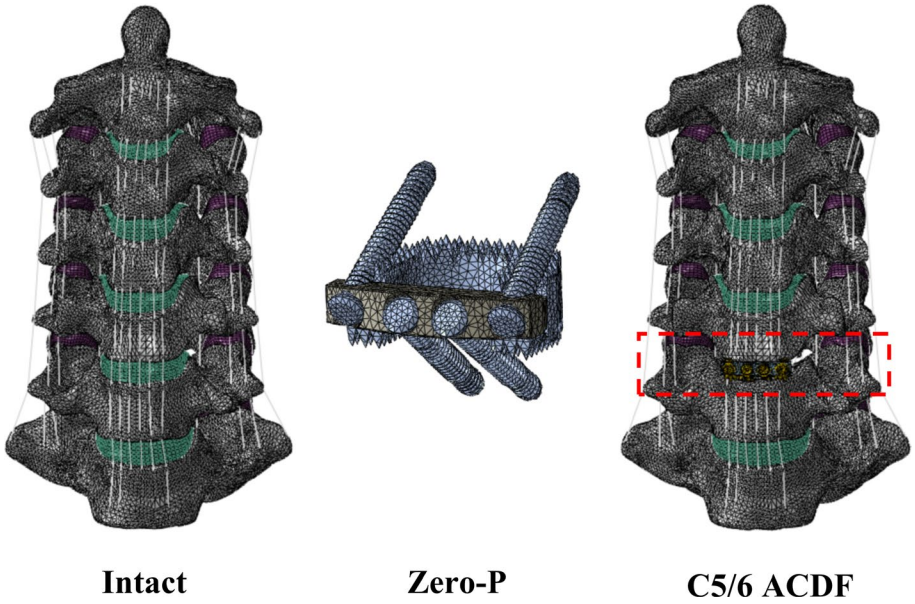

FIGURE 1 | Finite element model of a healthy cervical spine (C2–C7) and a C5/6 surgical model.

TABLE 1 | Material properties.

	Yong modulus (MPa)	Poisson's ratio
Cortical bone	12,000	
Cancellous bone	450	0.29
Annulus fibers	110	0.3
Nucleus pulposus	1	0.49
Cartilage	10.4	0.4
Endplate	500	0.25
ALL	10	0.3
PLL	10	0.3
CL	10	0.3
LF	1.5	0.3
IL	1.5	0.3
SL	1.5	0.3
Titanium	110,000	0.3
PEEK	3600	0.3

Abbreviations: ALL, anterior longitudinal ligament; CL, capsular ligament; IL, interspinous ligament; LF, ligamentum flavum; PLL, posterior longitudinal ligament; SL, supraspinous ligament.

Nonbonded contact was established between the pertinent vertebral surfaces and the supra- and infra-adjacent surfaces of the cage using a contact friction coefficient of 0.3. To mimic stiff fusion and adequate osseointegration, tie constraints were applied to the screw- and graft-vertebra interfaces. Shared nodes at the screw–plate interfaces were employed to simplify the model, thus preventing relative motion between the parts [18, 20, 21].

2.2 | Biomechanical Testing

To simulate the movement of the human cervical spine, finite element (FE) models were fixed at the inferior endplate of C7, and follower loads of 75 N were applied to replicate muscle force and head weight. A 1.0 N·m moment was applied to the top of C2 to produce flexion, extension, lateral bending, and axial rotation. We subsequently observed the following indicators: (1) the maximum stress of the vertebra at the operative segment and adjacent segments in the models with different implant heights; (2) the maximum stress of the intervertebral disc and facet joints at the operative segment and adjacent segments in different implant height models; and (3) the size and stress distribution of the zero-profile implant screw, titanium plate, cage, and bone interface. In addition, the range of motion (ROM) of the segments was recorded and compared with published studies to verify the validity of the models in the study.

3 | Results

3.1 | Validation of the Developed FE Models

The intact cervical spine finite element model constructed in this study contains 624,791 units and 420,173 nodes, meeting the accuracy requirements of the study. After a 75 N preload was applied, a 1 N·m moment was applied to the cervical spine across 6° degrees of freedom (flexion, extension, left and right lateral bending, and left and right rotation). The ROM of each segment in these 6° of freedom was measured. The ROM measurements for the C2/3 segment during flexion, extension, lateral bending, and rotation were 4.42°, 3.87°, 8.68°, and 11.25°, respectively. For the C3/4 segment, the values were 3.98°, 5.30°, 10.27°, and 8.07°; for the C4/5 segment, they were 4.83°, 5.07°, 12.81°, and 10.81°; for the C5/6 segment, they were 4.57°, 5.17°, 12.25°, and 8.59°; and for the C6/7 segment, the values were 3.59°, 4.53°, 9.08°, and

8.76°. These results were compared with those of previous studies and were found to be within the normal range, demonstrating that the model has a high degree of fit and is both accurate and reliable (Figure 2).

3.2 | Stress of the Vertebrae

The results indicated that the maximum stress on the vertebral body in the surgical segment under self-weight increased with increasing height of the implanted Zero-P device. Compared with the M1 model, the M4 model presented the highest maximum stress on the C5 vertebrae under self-weight, increasing by 231.2%, whereas the M2 model presented the highest maximum stress on the C6 vertebrae under self-weight, increasing by 290.3%. Under six different loading conditions, the maximum stress on the vertebral body in the surgical segment of the M4 model was generally greater than that in the M2 and M3 models. (Figure 3).

For the C4 vertebra, which represented the upper adjacent segment, the M1 model group presented the smallest maximum stress values under self-weight and six loading conditions. Conversely, the M4 model had the highest maximum stress values under flexion, extension, left bending, left and right rotation, and self-weight conditions, which increased by 50.8%, 65.0%, 62.3%, 121.0%, 119.2%, and 135.9%, respectively, compared with those of the M1 model. The M2 model displayed the highest maximum stress value of the C4 vertebra under right bending, which was 73.0% greater than that of the M1 model. For the C7 vertebra, which represented the lower adjacent segment, the M2 model demonstrated the highest maximum stress values in flexion, extension, right bending, left and right rotation, and self-weight conditions, which increased by 25.0%, 26.9%, 24.7%, 8.1%, 56.4%, and 1.2%, respectively, compared with those of the M1 model. The smallest maximum stress value in the left bend occurred in the M2 model and decreased by 4.6% compared with that in the M1 model. Compared with the M1 model, the M3 model presented the lowest maximum stress values in the flexion, extension, right bending, left and right rotation, and self-weight conditions, which were 65.7%, 16.9%, 33.9%, 8.1%, 19.2%, and 16.0%, respectively (Figure 3).

3.3 | Stress of the Adjacent Intervertebral Discs

Under self-weight conditions, the maximum stress of the C4/5 intervertebral disc in the M1 model was 2.792 MPa, and the maximum stress of the C6/7 intervertebral disc was 2.424 MPa. Following an increase in the height of the implant from 6 mm to 8 mm, the maximum stress of the C4/5 intervertebral disc increased by 21.6%, and the maximum stress of the C6/7 intervertebral disc increased by 11.9%. In the M4 model, the intervertebral disc stress of both segments reached its peak. Under different loading conditions, the maximum stress values of the intervertebral discs of these segments increase during extension and left and right bending, whereas the maximum stress values decrease during flexion (Figure 4).

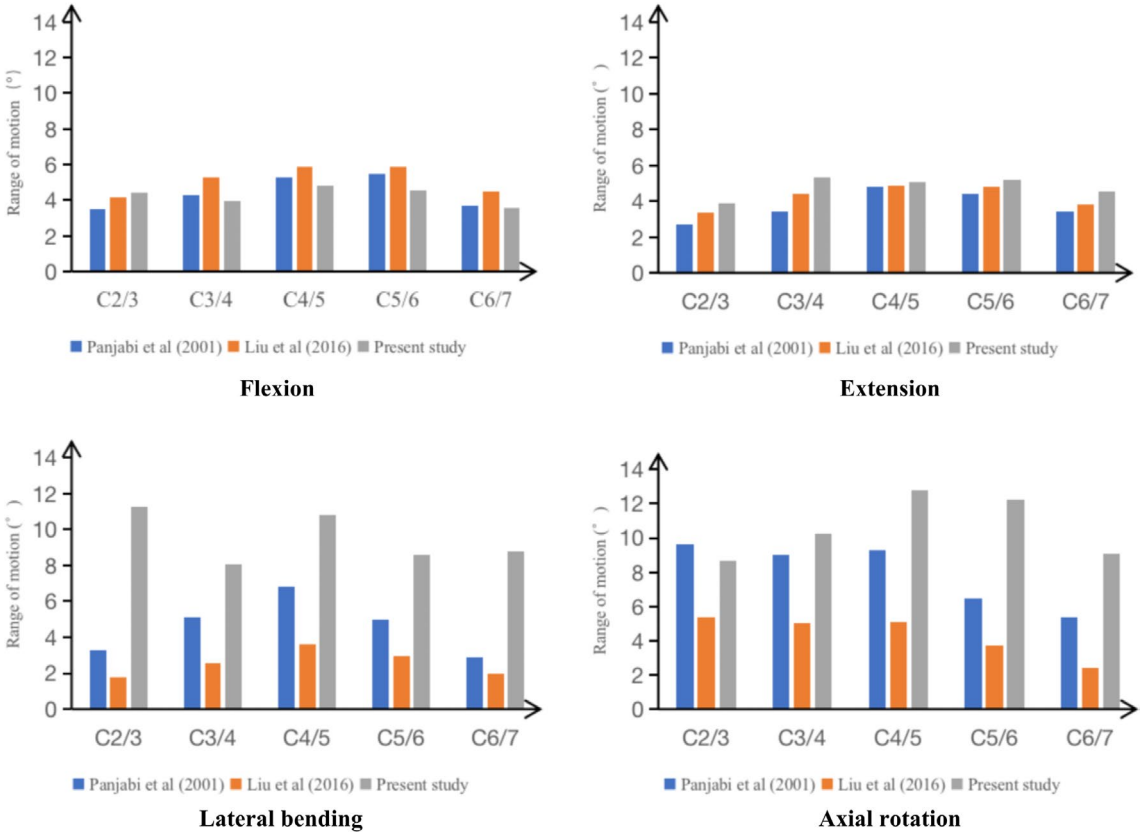

FIGURE 2 | Validation of the intact finite element model on the basis of previously published studies.

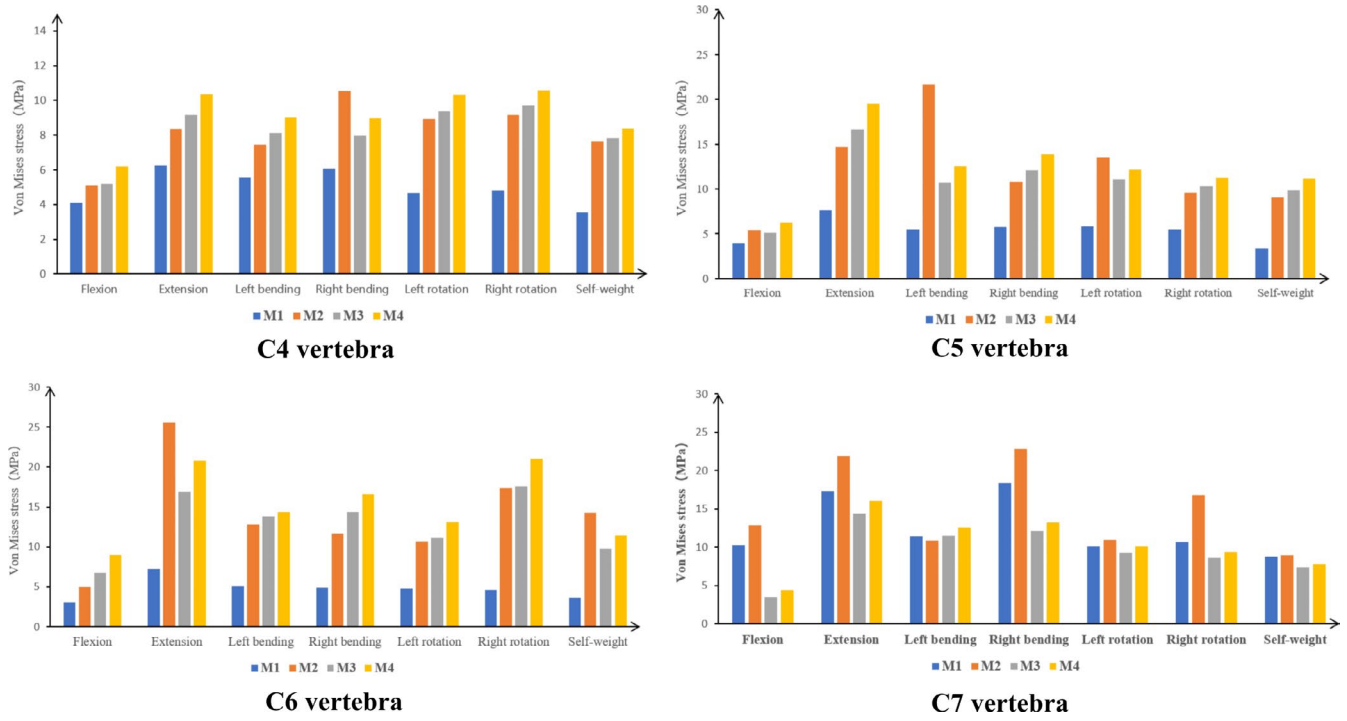

FIGURE 3 | The maximum stress on the vertebral body of the surgical segment and adjacent segments.

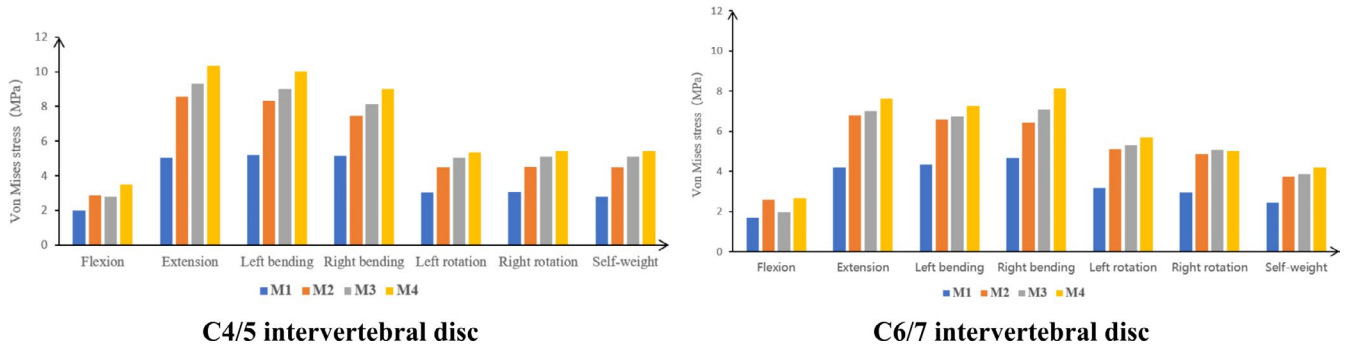

FIGURE 4 | The maximum stress of the adjacent intervertebral disc.

3.4 | Stress of the Zero-P Implant

In the three surgical models, the maximum stress generated by Zero-P implants of varying heights after intervertebral implantation differed significantly. In the M4 model, the implant experienced the highest stress, whereas the M2 model exhibited the lowest stress on the implant under both self-weight and six different loading conditions. Specifically, with increasing implant height from 6 mm to 8 mm, the maximum stress increased by 245.0% under self-weight, 363.0% under flexion, 195.2% under extension, 679.2% under left flexion, 135.2% under right flexion, 435.9% under left rotation, and 59.6% under right rotation. The M3 model's stress levels fall between those of the M2 and M4 models (Figure 5).

3.5 | Stress of the Facet Joints

Additionally, the stress on the posterior facet joints of the surgical segment increased with increasing height of the Zero-P implant. Under self-weight, extension, left and right bending, and left and right rotation, the superior facet joint stress in the M4 model increased by 55.6%, 57.9%, 54.4%, 52.4%, 78.1%, and 115.1%, respectively, and the inferior facet joint stress increased by 70.8%, 69.7%, 49.0%, 67.0%, 63.0%, and 56.7%, respectively, compared with that in the M2 model. The range of maximum stress on the posterior facet joints for the M3 model was situated between that of the M2 and M4 models. However, during flexion, the maximum stresses on the superior and inferior bilateral facet joints in the M3 model were 0.146 MPa and 0.106 MPa, respectively, which were greater than the stresses on the facet joints in the M2 and M4 models under the same conditions (Figure 6).

Under the self-weight condition, an increase in the height of the device corresponded with a gradual increase in the stress experienced by the upper and lower adjacent facet joints. For the superior part of the C4/5 facet joint, the stress values are maximal in the extension state, with the M2 model showing 1.115 MPa, the M3 model showing 1.252 MPa, and the M4 model showing 1.407 MPa. Conversely, these values are minimal in the flexion state, with values of 0.0006 MPa, 0.0004 MPa, and 0.0008 MPa

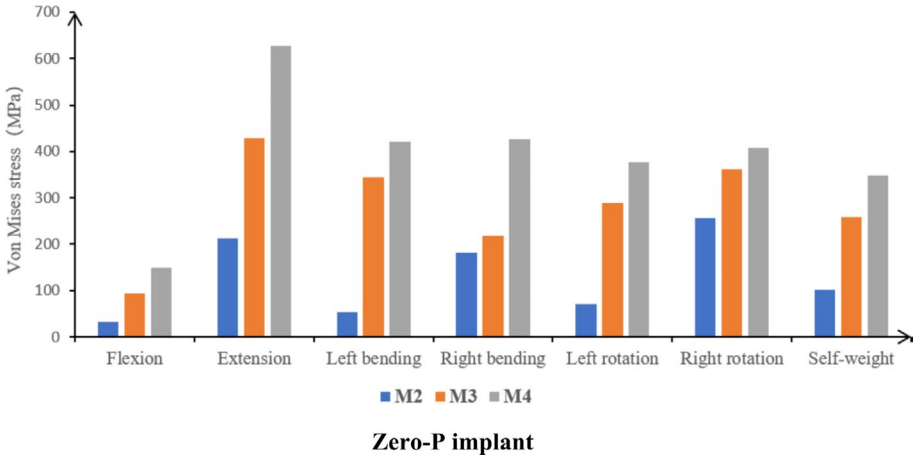

FIGURE 5 | The maximum stress of the Zero-P implant.

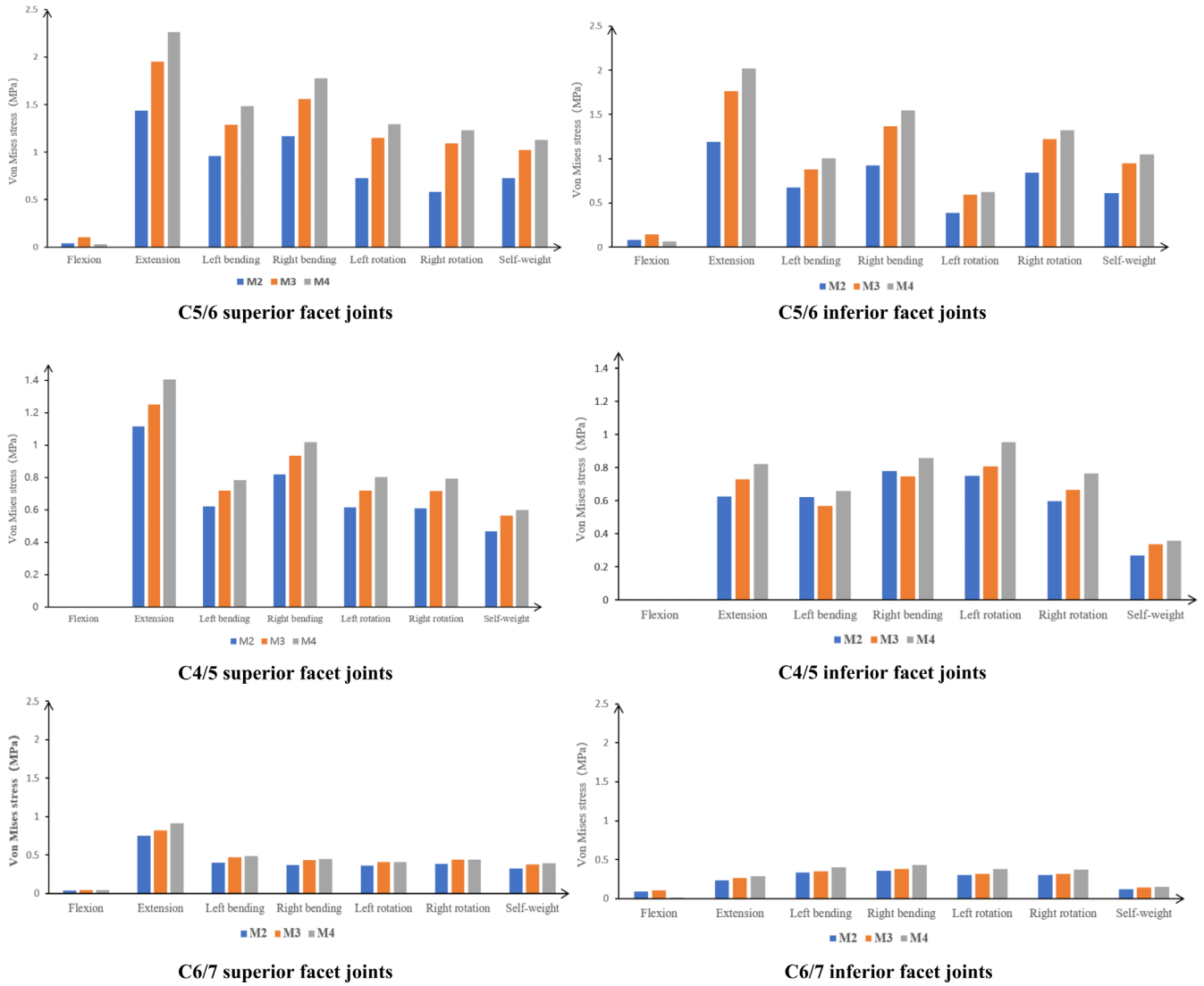

FIGURE 6 | The maximum stress on the posterior facet joints of the surgical segment and adjacent segments.

for the M2, M3, and M4 models, respectively. Similarly, for the inferior part of the C4/5 facet joint, the stress values are minimized in the flexion state, with readings of 0.0004 MPa, 0.0004 MPa, and 0.0005 MPa for the M2, M3, and M4 models, respectively. However, the stress value for the M2 model is highest during right flexion, whereas the M3 and M4 models exhibit

peak stresses during left rotation. For the C6/7 facet joints, the stress values are greatest in the extension state and smallest in the flexion state across all the models. Similarly, the stress values in the lower C6/7 facet joints are highest during right flexion and lowest during flexion (Figure 6). All stress nephograms are presented in Figure S1.

4 | Discussion

Under normal physiological conditions, the anterior column of the cervical spine bears approximately one-third of the axial stress, whereas the posterior column bears the remaining axial stress [23]. During the progression of cervical spondylosis, degenerative changes lead to pathological alterations such as loss of the physiological curvature of the cervical spine, narrowing of the intervertebral space, osteophyte formation, and disc herniation [24, 25]. These changes significantly impact the biomechanical environment of the functional spinal unit (FSU) [25]. Implanting an intervertebral implant of appropriate height can restore the intervertebral height and improve the degree of cervical sagittal alignment [26, 27]. Therefore, in addition to achieving decompression, the aim of ACDF surgery should be to reconstruct the biomechanical environment of the normal cervical FSU as much as possible. Excessive distraction of the surgical intervertebral disc space increases the stress on the posterior facet joint and the adjacent segment intervertebral disc, altering the normal biomechanical environment of the FSU [28, 29]. Consequently, selecting an appropriately sized intervertebral fusion cage to further optimize and improve the surgical outcomes of ACDF has been a focal point of scholarly discussion [30–33].

A retrospective study conducted by Wang et al. [34] elucidated the influence of the cage size of the Zero-profile implant system on surgical and radiological outcomes following ACDF. The research results indicated that if both adjacent sizes of Zero-profile implants fit the disc space adequately, a slightly larger height without being oversized may be a better choice for ensuring a satisfactory long-term prognosis. This is because it can maintain cervical sagittal balance and FSU height while promoting early bone fusion. Although the above conclusion strongly supports the findings of this study, as a clinical investigation, it did not examine the changes in force distribution on adjacent segmental vertebrae, intervertebral discs, and facet joints nor did it assess the impact on the overall biomechanical environment of the cervical spine. Therefore, three-dimensional FE analysis was utilized to investigate the biomechanical effects of different sizes of Zero-P implants on both the surgical segment and adjacent segments post-implantation in this study.

In this study, under different loading conditions, as the height of the Zero-P devices increased, the stress on the upper and lower vertebrae of the surgical segment correspondingly increased compared with that of the intact cervical spine model. The findings presented above are consistent with those reported in previous studies [28, 35]. Zhang et al. [28] established an ACDF surgical model of the C4/5 segment and analyzed the effects of different bone graft heights. When the implant height was 6.6 mm, the maximum stresses on the surgical segment during flexion, extension, rotation, and lateral bending were 52%, 66%, 63%, and 63%, respectively, of those observed at an implant height of 8.8 mm. Wen et al. [36] conducted in vitro biomechanical experiments using cadaveric specimens and reported that when the intervertebral space was stretched to 6–7 mm, the surgical segment entered an overdistraction state, causing the distraction force required for further dilation to increase substantially. Using a cage of an appropriate height avoids excessive distraction of the intervertebral space in the surgical segment, resulting in less stress on the vertebral body and a more even distribution of intervertebral stress. This even distribution helps facilitate the formation of a bony connection between the bone graft in the cage and the upper and lower end plates. Conversely, implanting a cage that is too tall will overly expand the intervertebral space of the surgical segment, generating greater stress. This increased stress can damage the cage and bony end plates, increasing the risks of cage subsidence, intervertebral space collapse, and delayed bony fusion [36–38]. Additionally, the maximum stress on the Zero-P devices in the surgical model gradually increased with increasing height in this study, as the Zero-P implant bears the stress of the surgical segment before bony fusion is achieved.

In this study, we observed that the stress on the upper and lower adjacent cervical intervertebral discs increased with increasing height of the implanted Zero-P under self-weight conditions. Under the six loading conditions, the stress on the adjacent segment intervertebral discs significantly increased in the extension, left flexion, and right flexion states, whereas the stress in the flexion state was lower than that under self-weight conditions. Moreover, the maximum stress on the C7 vertebra under self-weight conditions did not significantly increase with increasing height of the implanted Zero-P. However, the maximum stress on the C4 vertebra under self-weight conditions significantly increased with increasing height of the implant. This finding indicates a differential impact on the upper and lower adjacent segments on the basis of the height of the implant, highlighting the importance of selecting a device of an appropriate height to minimize stress and potential degeneration in adjacent segments.

The bilateral facet joints at the back of the cervical spine and the anterior intervertebral disc together form a three-joint complex [19]. Previous studies have shown that approximately 23% of the axial load is transmitted through the posterior facet joints during cervical spine movement [39]. The stress on the posterior facet joints of the surgical segment increased with increasing height of the Zero-P implant under different loading conditions in this study. Excessive distraction of the facet joints is closely related to postoperative neck pain. A study by Ye et al. [40]. showed that when the facet joint distance was greater than 0.905 mm, the probability of postoperative neck pain significantly increased. Ha et al. [32]. suggested that the torque of intraoperative distraction should not exceed 6.0 kgf·cm to help reduce the incidence of early neck pain in patients after ACDF surgery. Therefore, when the intervertebral height of the FSU is restored, the facet joints should not be overdistracted [29, 39]. As the height of the Zero-P increases, the distance between the posterior facet joints also increases, reducing the overlap between the facet joints. This reduction in overlap results in increased stress on the bilateral facet joints at the back of the surgical segment, reaching its maximum value in the extension state. Concurrently, the stress on the facet joints of adjacent

segments also increases. Additionally, patients who undergo ACDF should avoid excessive activity in the early postoperative period to prevent an abnormal increase in pressure in the facet joints, particularly during neck extension movements.

To determine the appropriate height of an implant, the mean height of the intervertebral space within the surgical segment can serve as a reference for establishing upper and lower boundaries during ACDF, such as the range of 6 mm–7 mm used in this study [15]. Thus, we recommend choosing a larger implant on the basis of this study. In cases of severe degeneration or stenosis at the surgical segment, the average preoperative intervertebral disc height of adjacent segments can serve as a reliable reference [15]. This can ensure that the contact surface between the implant and bone maintains a consistent level of pressure while avoiding excessive expansion of the intervertebral space during surgery, which can help maintain the sagittal balance of the cervical spine after surgery and promote early bony fusion. However, it is important to avoid selecting an oversized Zero-P device, as it can increase the maximum stress on the vertebral body of the surgical segment, the implant itself, the posterior facet joints, and the intervertebral discs of adjacent segments. This heightened stress is particularly evident under various activity states, potentially adversely affecting the long-term prognosis following ACDF surgery.

4.1 | Limitations

The current study has several limitations that warrant consideration. First, the study was conducted using a single FE model, which may only yield a simulated result that is not necessarily representative of the actual in vivo conditions. Second, as discussed earlier, the results of calculating the appropriate range of Zero-P height using the average of adjacent segmental values need to be further validated. Third, we specifically chose the C5/6 as the surgical segment (commonly affected in cervical degenerative disc disease), recognizing that this may not fully replicate all clinical scenarios but serves as a benchmark for directional changes. Furthermore, this study exclusively examines single-segment ACDF, highlighting the necessity for additional research on multi-segment surgeries. Thus, further in vitro and in vivo studies are warranted to validate these findings.

5 | Conclusions

In general, after the appropriate range in implant height has been determined on the basis of the mean height of the intervertebral space, a larger size Zero-P should be selected. This approach helps maintain the intervertebral space height while providing greater stress, which facilitates tighter fitting of the upper and lower bony end plates with the implant. Such a fit is beneficial for maintaining postoperative cervical sagittal balance and promoting early bony fusion. Simultaneously, this approach avoids the complications associated with implanting a Zero-P that is oversized, such as increased maximum stress on the vertebral body of the surgical segment, the implant itself, the posterior facet joint, and the intervertebral discs of adjacent segments. Excessive stress in these areas, particularly under different activity states, can negatively impact patients' long-term prognoses following ACDF surgery.

Author Contributions

All authors contributed to the study conception and design. Concepts and funding sources were provided by [Cheng-yi Huang] and [Hao Liu]. Surgical and perioperative nursing care were provided by [Hao Liu], [Chengyi Huang] and [Jun-bo He]. Material preparation, data collection and analysis were performed by [Cheng-yi Huang], [Xing-Jin Wang] and [Ting-kui Wu]. The first draft of the manuscript was written by [Chengyi Huang], [Tingkui Wu] and reviewed by [Hao Liu], [Bei-yu Wang] and [Jin Xu]. All authors read and approved the final manuscript.

Acknowledgments

The study was funded by research grants from the Cadre Health Research Project of Sichuan Province (Grant no ZH2023-105 to Hao Liu); the National Natural Science Foundation of China (Grant no 82302785 to Ting-kui Wu); the 1.3.5 project for Postdoctoral Foundation of West China Hospital of Sichuan University (Grant no 2023HXBH080 to Ting-kui Wu).

Ethics Statement

The study protocol was approved by the institutional ethics committee of West China Hospital of Sichuan University and in accordance with the 1964 Helsinki Declaration and its later amendments or comparable ethical standards (Project License Number 20190946).

Consent

All patients signed informed consent prior to study participation.

Conflicts of Interest

The authors declare no conflicts of interest.

References

1. G. R. Buttermann, "Anterior Cervical Discectomy and Fusion Outcomes Over 10 Years: A Prospective Study," *Spine (Phila Pa 1976)* 43, no. 3 (2018): 207–214.

2. P. Y. Joo, J. R. Zhu, A. J. Kammien, M. J. Gouzoulis, P. M. Arnold, and J. N. Grauer, "Clinical Outcomes Following One-, Two-, Three-, and Four-Level Anterior Cervical Discectomy and Fusion: A National Database Study," *Spine Journal* 22, no. 4 (2022): 542–548.

3. C. D. Lopez, V. Boddapati, J. M. Lombardi, et al., "Recent Trends in Medicare Utilization and Reimbursement for Anterior Cervical Discectomy and Fusion," *Spine Journal* 20, no. 11 (2020): 1737–1743.

4. E. Chong, M. H. Pelletier, R. J. Mobbs, and W. R. Walsh, "The Design Evolution of Interbody Cages in Anterior Cervical Discectomy and Fusion: A Systematic Review," *BMC Musculoskeletal Disorders* 16 (2015): 99.

5. X. Q. Sheng, Y. Yang, C. Ding, et al., "Uncovertebral Joint Fusion Versus End Plate Space Fusion in Anterior Cervical Spine Surgery: A Prospective Randomized Controlled Trial," *Journal of Bone and Joint Surgery. American Volume* 105, no. 15 (2023): 1168–1174.

6. J. D. Oliver, S. Goncalves, P. Kerezoudis, et al., "Comparison of Outcomes for Anterior Cervical Discectomy and Fusion With and Without Anterior Plate Fixation," *Spine* 43, no. 7 (2018): E413–E422.

7. Y. Zhao, S. Yang, Y. Huo, Z. Li, D. Yang, and W. Ding, "Locking Stand-Alone Cage Versus Anterior Plate Construct in Anterior Cervical Discectomy and Fusion: A Systematic Review and Meta-Analysis Based on Randomized Controlled Trials," *European Spine Journal* 29, no. 11 (2020): 2734–2744.

8. W. Hua, J. Zhi, W. Ke, et al., "Adjacent Segment Biomechanical Changes After One- or Two-Level Anterior Cervical Discectomy and Fusion Using Either a Zero-Profile Device or Cage Plus Plate: A Finite Element Analysis," *Computers in Biology and Medicine* 120 (2020): 103760.

9. C. Huang, H. Abudouaini, B. Wang, et al., "Comparison of Patient-Reported Postoperative Dysphagia in Patients Undergoing One-Level Versus Two-Level Anterior Cervical Discectomy and Fusion With the Zero-P Implant System," *Dysphagia* 36, no. 4 (2021): 743–753.

10. M. Scholz, P. Schleicher, S. Pabst, and F. Kandziora, "A Zero-Profile Anchored Spacer in Multilevel Cervical Anterior Interbody Fusion: Biomechanical Comparison to Established Fixation Techniques," *Spine (Phila Pa 1976)* 40, no. 7 (2015): E375–E380.

11. M. Scholz, P. M. Reyes, P. Schleicher, et al., "A New Stand-Alone Cervical Anterior Interbody Fusion Device: Biomechanical Comparison With Established Anterior Cervical Fixation Devices," *Spine (Phila Pa 1976)* 34, no. 2 (2009): 156–160.

12. K. N. Fountas, E. Z. Kapsalaki, L. G. Nikolakakos, et al., "Anterior Cervical Discectomy and Fusion Associated Complications," *Spine (Phila Pa 1976)* 32, no. 21 (2007): 2310–2317.

13. Z. Sun, Z. Liu, W. Hu, Y. Yang, X. Xiao, and X. Wang, "Zero-Profile Versus Cage and Plate in Anterior Cervical Discectomy and Fusion With a Minimum 2 Years of Follow-Up: A Meta-Analysis," *World Neurosurgery* 120 (2018): e551–e561.

14. T. Zhang, N. Guo, G. Gao, et al., "Comparison of Outcomes Between Zero-p Implant and Anterior Cervical Plate Interbody Fusion Systems for Anterior Cervical Decompression and Fusion: A Systematic Review and Meta-Analysis of Randomized Controlled Trials," *Journal of Orthopaedic Surgery and Research* 17, no. 1 (2022): 47.

15. C. Wu, X. Yang, X. Gao, et al., "The Effects of Cages Implantation on Surgical and Adjacent Segmental Intervertebral Foramina," *Journal of Orthopaedic Surgery and Research* 16, no. 1 (2021): 280.

16. W. Xiong, J. Zhou, C. Sun, et al., "0.5- to 1-Fold Intervertebral Distraction Is a Protective Factor for Adjacent Segment Degeneration in Single-Level Anterior Cervical Discectomy and Fusion," *Spine (Phila Pa 1976)* 45, no. 2 (2020): 96–102.

17. C. H. Cheng, P. Y. Chiu, H. B. Chen, C. C. Niu, and M. Nikkhoo, "The Influence of Over-Distraction on Biomechanical Response of Cervical Spine Post Anterior Interbody Fusion: A Comprehensive Finite Element Study," *Frontiers in Bioengineering and Biotechnology* 11 (2023): 1217274.

18. K. Huang, Q. Wang, X. Rong, et al., "Biomechanical Effects on the Prostheses and Vertebrae of Three-Level Hybrid Surgery: A Finite Element Study," *Orthopaedic Surgery* 16 (2024): 2019–2029.

19. X. Rong, B. Wang, C. Ding, et al., "The Biomechanical Impact of Facet Tropism on the Intervertebral Disc and Facet Joints in the Cervical Spine," *Spine Journal* 17, no. 12 (2017): 1926–1931.

20. T. K. Wu, Y. Meng, H. Liu, et al., "Biomechanical Effects on the Intermediate Segment of Noncontiguous Hybrid Surgery With Cervical Disc Arthroplasty and Anterior Cervical Discectomy and Fusion: A Finite Element Analysis," *Spine Journal* 19, no. 7 (2019): 1254–1263.

21. Y. W. Shen, Y. Yang, H. Liu, et al., "Biomechanical Evaluation of Intervertebral Fusion Process After Anterior Cervical Discectomy and Fusion: A Finite Element Study," *Frontiers in Bioengineering and Biotechnology* 10 (2022): 842382.

22. T. K. Wu, H. Liu, B. Y. Wang, et al., "Incidence of Bone Loss After Prestige-LP Cervical Disc Arthroplasty: A Single-Center Retrospective Study of 396 Cases," *Spine Journal* 20, no. 8 (2020): 1219–1228.

23. G. P. Pal and H. H. Sherk, "The Vertical Stability of the Cervical Spine," *Spine (Phila Pa 1976)* 13, no. 5 (1988): 447–449.

24. D. Shedid and E. C. Benzel, "Cervical Spondylosis Anatomy: Pathophysiology and Biomechanics," *Neurosurgery* 60, no. 1 Suppl 1 (2007): S7–S13.

25. T. N. Degenerative and C. Spondylosis, "Degenerative Cervical Spondylosis," *New England Journal of Medicine* 383, no. 2 (2020): 159–168.

26. T. Yamagata, T. Takami, T. Uda, et al., "Outcomes of Contemporary Use of Rectangular Titanium Stand-Alone Cages in Anterior Cervical Discectomy and Fusion: Cage Subsidence and Cervical Alignment," *Journal of Clinical Neuroscience* 19, no. 12 (2012): 1673–1678.

27. H. Yoshihara, "Indirect Decompression in Spinal Surgery," *Journal of Clinical Neuroscience* 44 (2017): 63–68.

28. Y. Zhang, J. Zhou, X. Guo, Z. Cai, H. Liu, and Y. Xue, "Biomechanical Effect of Different Graft Heights on Adjacent Segment and Graft Segment Following C4/C5 Anterior Cervical Discectomy and Fusion: A Finite Element Analysis," *Medical Science Monitor* 25 (2019): 4169–4175.

29. X. F. Wang, Y. Meng, H. Liu, B. Y. Wang, and Y. Hong, "The Impact of Different Artificial Disc Heights During Total Cervical Disc Replacement: An In Vitro Biomechanical Study," *Journal of Orthopaedic Surgery and Research* 16, no. 1 (2021): 12.

30. M. H. Lawless, E. J. Yoon, J. M. Jasinski, et al., "Impact of Interspace Distraction on Fusion and Clinical Outcomes in Anterior Cervical Discectomy and Fusion: A Longitudinal Cohort Study," *Asian Spine Journal* 16, no. 3 (2022): 369–374.

31. J. S. Lee, D. W. Son, S. H. Lee, et al., "The Effect of Hounsfield Unit Value With Conventional Computed Tomography and Intraoperative Distraction on Postoperative Intervertebral Height Reduction in Patients Following Stand-Alone Anterior Cervical Discectomy and Fusion," *Journal of Korean Neurosurgical Association* 65, no. 1 (2022): 96–106.

32. S. M. Ha, J. H. Kim, S. H. Oh, J. H. Song, H. I. Kim, and D. A. Shin, "Vertebral Distraction During Anterior Cervical Discectomy and Fusion Causes Postoperative Neck Pain," *Journal of Korean Neurosurgical Association* 53, no. 5 (2013): 288–292.

33. Y. Y. Yi, H. Chen, H. W. Xu, S. B. Zhang, and S. J. Wang, "Changes in Intervertebral Distraction: A Possible Factor for Predicting Dysphagia After Anterior Cervical Spinal Surgery," *Journal of Clinical Neuroscience* 100 (2022): 82–88.

34. X. J. Wang, J. B. He, T. K. Wu, et al., "The Influence of Zero-Profile Implant Selection on the Outcomes of Anterior Cervical Discectomy and Fusion," *Orthopaedic Surgery* (2024).

35. E. Truumees, C. K. Demetropoulos, K. H. Yang, and H. N. Herkowitz, "Effects of Disc Height and Distractive Forces on Graft Compression in an Anterior Cervical Discectomy Model," *Spine (Phila Pa 1976)* 27, no. 22 (2002): 2441–2445.

36. J. Wen, J. Xu, L. Li, et al., "Factors Affecting the Nonlinear Force Versus Distraction Height Curves in an In Vitro C5–C6 Anterior Cervical Distraction Model," *Clinical Spine Surgery* 30, no. 5 (2017): E510-e4.

37. H. Igarashi, M. Hoshino, K. Omori, et al., "Factors Influencing Interbody Cage Subsidence Following Anterior Cervical Discectomy and Fusion," *Clinical Spine Surgery* 32, no. 7 (2019): 297–302.

38. D. Z. Yin, X. T. Xin, R. Yang, Y. P. Shi, and H. Y. Shen, "Biomechanical Stability of Lower Cervical Spine Immediately After Discectomy With Grafting," *Orthopaedic Surgery* 3, no. 2 (2011): 113–118.

39. G. P. Pal and R. V. Routal, "A Study of Weight Transmission Through the Cervical and Upper Thoracic Regions of the Vertebral Column in Man," *Journal of Anatomy* 148 (1986): 245–261.

40. W. Ye, Z. Wang, Y. Zhu, and W. Cai, "Analysis of Functional Outcomes and Risk Factors for Facet Joint Distraction During Anterior Cervical Discectomy and Fusion for Cervical Spondylotic Myelopathy," *World Neurosurgery* 162 (2022): e301–e308.

Supporting Information

Additional supporting information can be found online in the Supporting Information section.